Inorg. Chem. **2008**, *47*, 3023−3033

Molecular Structures of the Digermanes $Me_2XGeGeXMe_2$ (X = Me, Cl, and H): An Ab Initio Study Combined with Experimental Investigation by Raman Spectroscopy and Gas Electron Diffraction

Margit Hölbling,[†] Sarah L. Masters (née Hinchley),[*,‡] Michaela Flock,[†] Judith Baumgartner,[†] Karl Hassler,[†] Heather E. Robertson,[‡] and Derek A. Wann[‡]

Institut für Anorganische Chemie, Technische Universität Graz, Stremayrgasse 16, A-8010 Graz, Austria, and School of Chemistry, University of Edinburgh, West Mains Road, Edinburgh, EH9 3JJ, Scotland

Received September 21, 2007

Ab initio calculations were carried out to investigate the potential-energy surface for internal rotation of the methylated digermanes hexamethyldigermane $Me_3GeGeMe_3$ (**1**), dichlorotetramethyldigermane $Me_2ClGeGeClMe_2$ (**2**), and tetramethyldigermane $Me_2HGeGeHMe_2$ (**3**). Different basis sets [6–31+G(d), SDD, aug-cc-pVTZ] were employed at the DFT and MP2 levels of theory to optimize structures and to calculate energies and vibrational frequencies. For **1**, one minimum representing a staggered structure was located on the potential-energy surface. For **2** and **3**, antiperiplanar conformations with C_2 symmetry were found to be the global minima. Additionally, synclinal minima were located for **2** and **3** when certain basis sets were employed. Determination of structural parameters in the gas phase by gas electron diffraction confirmed the computed predictions for all three compounds. For **2** and **3**, the ratios of antiperiplanar to synclinal conformer were detected to be 90:10 (328 K) and 72:28 (293 K), respectively, by gas electron diffraction. The experimentally determined GeGe bond lengths in **1**, **2**, and **3** in the gas phase are 241.4(1), 242.7(2) (averaged for antiperiplanar and synclinal), and 241.7(1) pm (equal for antiperiplanar and synclinal). Only averaged structures were observed, using Raman spectroscopy, for **2** and **3** because the wavenumber differences are small between conformers and there is only a small contribution from the second conformer in each case. For **2**, the crystal structure was also determined by X-ray diffraction. An anticlinal structure (with Cl atoms eclipsing the C atoms) was found with a GeGe bond length of 242.1 pm.

Introduction

The barriers to internal rotation around bonds between elements in group 14 decrease within the series C−C, Si−Si, Ge−Ge, and further to Sn−Sn and Pb−Pb. Although the most investigated system in terms of conformations and barriers is ethane and its derivatives, disilane has also been extensively studied. For instance, while the rotational barrier in ethane is ∼12.2 kJ mol^{-1},[1] for disilane, it was determined to be only 5.1 kJ mol^{-1}.[2] For hexamethyldisilane, $Me_3SiSiMe_3$, Schleyer et al. reported a barrier of only ∼4 kJ mol^{-1} (MP2/6–31G*//6–31G*), which is almost the same as for disilane.[3] However, recent NMR spectroscopic reinvestigations found a higher rotational barrier for $Me_3SiSiMe_3$ of ∼7 kJ mol^{-1}.[4]

More complex disilanes, such as Me_3SiSiH_3, MeX_2SiSiX_2Me with X = H, F, Cl, Br, and I, $ClMe_2SiSiMe_2Cl$,[5–7] and disilanes substituted with bulky ^{t}Bu groups, for example, ^{t}BuH_2SiSi$H_2{}^t$Bu, ^{t}Bu$_2$HSiSiH^{t}Bu$_2$, and ^{t}BuX_2SiSi$X_2{}^t$Bu,[8–10] have been studied computationally, as

* To whom correspondence should be addressed. E-mail: s.masters@ed.ac.uk.
† Technische Universität Graz.
‡ University of Edinburgh.

(1) For instance, see: Eliel, E. L.; Wilen, S. H. *Stereochemistry of Organic Compounds*; Wiley: New York, 1994.
(2) Beagley, B.; Conrad, A. R.; Freeman, J. M.; Monaghan, J. J.; Norton, B. G.; Holywell, G. C. *J. Mol. Struct.* **1972**, *11*, 371–380.
(3) Schleyer, P.v.R.; Kaupp, M.; Hampel, F.; Bremer, M.; Mislow, K. *J. Am. Chem. Soc.* **1992**, *114*, 6791–6797.
(4) Aksnes, D. W.; Kimtys, L. *Acta Chem. Scand.* **1995**, *49*(10), 722–727.
(5) Mohamed, T. A. *J. Mol. Struct. (THEOCHEM)* **2003**, *635*, 161–172.
(6) Jähn, A.; Schenzel, K.; Zink, R.; Hassler, K. *Spectrochim. Acta Part A* **1999**, *55*, 2677.
(7) Kveseth, K. *Acta Chem. Scand.* **1979**, *A33*(6), 453–462.
(8) Hnyk, D.; Fender, R. S.; Robertson, H. E.; Rankin, D. W. H.; Brühl, M.; Hassler, K.; Schenzel, K. *J. Mol. Struct.* **1995**, *346*, 215–229.

10.1021/ic7018764 CCC: $40.75
Published on Web 03/18/2008

well as by Raman spectroscopy in the liquid state and by gas electron diffraction (GED) in the gaseous state. For $Me_2ClSiSiClMe_2$, the Si analogue of $Me_2ClGeGeClMe_2$ in the current investigation, the anti conformer was predicted to be the global minimum by RHF/SBK calculations with E_{rel} of the gauche conformer being 5.4 kJ mol^{-1}.[7] This was verified by Raman spectroscopy for both the solid and liquid states (solid, anti conformer only; liquid, $E_{rel,gauche} = 4.2$ kJ mol^{-1}).[6] In the gas phase, however, the gauche conformer was found to be the most stable by GED.[7]

In the study of the conformations and rotational barriers of the whole series H_3XYH_3 (X, Y = C, Si, Ge, Sn, and Pb), Schleyer et al. predicted that the rotational barriers decrease from ~11 to ~1 kJ mol^{-1} from C to Pb, but do not vanish.[3] They predicted the staggered conformer as the minimum [HF level employing 3–21G(d,p) for C, Si, and H and split-valence basis sets of Huzinaga for Ge, Sn, and Pb]. Song et al.[11] calculated the barriers to rotation of the same series of compounds and found them in agreement, with a lowering of the barrier from ~13 to ~1 kJ mol^{-1} at the MP2 level [employing the basis sets 6–31G(d) for C and Si and LanL2DZ(d) for Ge, Sn and Pb]. It was deduced that the barriers are dominated by steric repulsion. The hyperconjugative interaction between the X−H bonding orbitals and the vicinal Y−H antibonding orbitals plays a secondary role.[11] The internal rotation in digermane was also investigated by Goodman and co-workers at the MP2 level of theory, employing the 6–311G(3df,2p) basis set.[12] Using NBO analysis, they found that the "quantum superposition" (hyperconjugation between the germyl groups, σGe−H → σ*Ge−H) accounts for only ~40% of the barrier. This effect of hyperconjugation is smaller than the Boltzmann energy at ambient temperature and therefore insufficient to prevent digermane from free rotation about the Ge−Ge bond. The rotational barrier of ~3.3 kJ mol^{-1} results from bond weakening caused by steric repulsion in combination with the hyperconjugation.[12]

In a recent study, Urban et al. investigated the molecular structures, vibrational spectra and rotational barriers of C_2H_6, Si_2H_6, $SiGeH_6$, and Ge_2H_6 at the HF, MP2, B3LYP, and CISD levels, employing polarized triple-ζ basis sets.[13] Although the discrepancy between theory and experiment in determination of the Ge−Ge bond length in H_3GeGeH_3 has been discussed before,[14] geometries and rotational barriers were determined with acceptable accuracy at the MP2 and DFT level.[13] They found that the geometries compare well, although the central E−E bond is shortened when electron correlation is included for all except the Ge−Ge system. The B3LYP method gives agreeable results for the Ge_2H_6 geometry and vibrational frequencies, but the rotational barriers are underestimated.[13]

From a recent theoretical investigation of cyclohexagermane by Hölbling et al., it is known that the barriers for ring inversion calculated with B3LYP are very reasonable when relativistic effects for Ge are included.[15] Without these, the barriers are overestimated by a factor of 4.

The conformational properties and rotational barriers of the ethane analogues of Si, Ge, Sn, and Pb are well studied theoretically and, in the cases of Si and Ge, also experimentally. There are also numerous papers concerned with the investigation of substituted di-, tri-, and tetrasilanes and so forth. However, there is still a lack of information regarding more complex structures of substituted digermanes (not to mention the distannanes and diplumbanes). As for the substituted disilanes, more than one stable conformer is expected for substituted digermanes, although neither a quantum chemical nor experimental investigation of the rotational conformers of these molecules has yet been published. Therefore, we were interested in studying the conformational equilibria of methylated digermanes to learn about conformational equilibria and rotational barriers.

In this paper, we report the molecular structures and conformational properties of hexamethyldigermane, $Me_3GeGeMe_3$ (**1**), dichlorotetramethyldigermane, $Me_2ClGeGeClMe_2$ (**2**), and tetramethyldigermane, $Me_2HGeGeHMe_2$ (**3**). The combination of quantum chemical calculations with Raman spectroscopy (solid, liquid, and solution phase), X-ray diffraction (solid phase), and gas electron diffraction (gas phase) is used to gain information about rotational barriers and structures in all the phases.

Experimental Section

Synthesis. Compound **1** was prepared according to the method reported by Triplett and Curtis.[16] Potassium was melted in cyclohexane, and chlorotrimethylgermane was added dropwise over a period of 30 min. The solution was refluxed for 2 h and then decanted. The pure product was obtained by fractional distillation in a yield of 60%.

To synthesize **2**, a pure sample of **1** was allowed to react with concentrated sulfuric acid for 24 h at room temperature. When the gas evolution had stopped, ammonium chloride was added in small portions, while the mixture was cooled in an ice bath. The solution was then stirred for 30 min, and the precipitate which had formed was separated and dissolved in pentane. Pure **2** was obtained by crystallization from pentane and subsequent sublimation (0.1 Torr/40 °C) in a yield of 85%.[16]

To prepare **3**, a procedure for Me_3SiSiH_3 (reduction of $Me_3SiSiCl_3$ with $LiAlH_4$ in di-*n*-butylether) was adapted.[17] A solution of **2** in dimethyltriglycol (triglyme, dried over a molecular sieve) was added dropwise to a dispersion of $NaBH_4$ in triglyme at 0 °C. The reaction was then stirred overnight at room temperature. Fractional distillation at 30 Torr/130 °C gave **3** as a colorless liquid

(9) Hinchley, S. L.; Robertson, H. E.; Parkin, A.; Rankin, D. W. H.; Tekautz, G.; Hassler, K. *Dalton Trans.* **2004**, *759*, 766.
(10) Hinchley, S. L.; Smart, B. A.; Morrison, C. A.; Robertson, H. E.; Rankin, D. W. H.; Coxall, R. A.; Parsons, S.; Zink, R.; Siegl, H.; Hassler, K.; Mawhorter, R. J. *J. Chem. Soc., Dalton Trans.* **2001**, *19*, 2916–2925.
(11) Song, L.; Lin, Y.; Wu, W.; Zhang, Q.; Mo, Y. *J. Phys. Chem. A* **2005**, *109*, 2310–2316.
(12) Goodman, L.; Pophoristic, V.; Wang, W. *Int. J. Quantum Chem.* **2002**, *90*, 657–662.
(13) Urban, J.; Schreiner, P. R.; Vacek, G.; Schleyer, P.v.R.; Huang, J. Q.; Leszczynski, J. *Chem. Phys. Lett.* **1997**, *264*, 441–448.
(14) Oberhammer, H.; Sundermeyer, W. *J. Mol. Struct.* **1994**, *323*, 125–128.
(15) Hölbling, M.; Lobreyer, T.; Flock, M.; Baumgartner, J.; Hassler, K. *Eur. J. Inorg. Chem.* **2007**, 4952–4957.
(16) Triplett, K.; Curtis, M. D. *J. Organomet. Chem.* **1976**, *107*, 23–32.
(17) Zink, R. PhD Dissertation, Universität Graz, Graz, Austria, 1997.

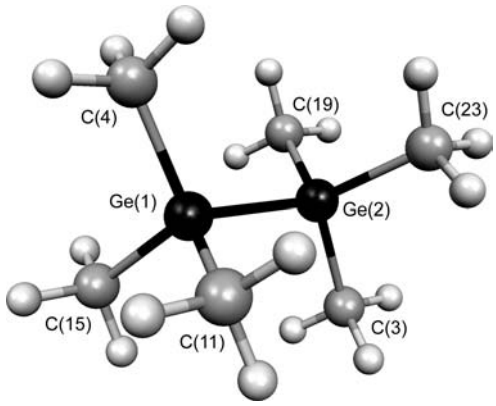

Figure 1. Molecular structure of $Me_3GeGeMe_3$ (**1**) showing a perspective view with atom numbering.

in a yield of 50%. The purity of all compounds was checked with ^1H and ^{13}C NMR and Raman spectroscopy, and the information was compared with literature data.[16]

Crystallography. The crystal structure of **2** was determined by mounting a crystal on the tip of a glass fiber. Data collection was performed with a BRUKER-AXS SMART APEX CCD diffractometer using graphite-monochromated Mo Kα radiation (0.71073 Å). The data were reduced to F_0^2 and corrected for absorption effects using SAINT[18] and SADABS,[19] respectively. The structure was solved by direct methods and refined by the full-matrix least-squares method (SHELXL97).[20] All non-hydrogen atoms were refined with anisotropic displacement parameters. All hydrogen atoms were located in calculated positions to correspond to standard bond lengths and angles.

Computational Methods. All geometry optimizations and energy minimizations, as well as the calculations of IR and Raman frequencies, were performed using the Gaussian03[21] package at the DFT and the MP2 levels of theory. Extensive searches of the torsional potentials of all three compounds were undertaken at the B3LYP and MP2 levels of theory, employing the SDD (hereafter referred to as basis set **A**) and 6–31+G* (**B**) basis sets to locate all minima. In some cases mixed basis sets were used, applying 6–31+G* to C, H, and Cl and SDD to Ge. These mixed basis sets are referred to as **A#**. The aug-cc-pVTZ-PP basis set for Ge, including quasi-relativistic Stuttgart Dresden effective-core potentials (ECP), and aug-cc-pVTZ for C, H, and Cl were employed for optimizations and energy calculations at the B3LYP level of theory only (**C**). The MP2 and B3LYP levels employing the same basis sets gave very similar results for geometry optimizations, as well as for energy calculations. Therefore, calculations including triple-ζ basis sets were only performed at the B3LYP level. Generally, all DFT calculations were performed using the B3LYP functional. For simplification, the methods will be referred to as DFT/basis set and compared to MP2/basis set. Vibrational frequency calculations were performed to determine the nature of the stationary points. Minima possess all real frequencies, while transition structures have a single, imaginary frequency. No symmetry restraints were used. Analytic second derivatives of the energy with respect to nuclear coordinates calculated for **1**, **2**, and **3** gave the force fields, which were used to provide estimates of the amplitudes of vibration (u_{h1})[22] and the curvilinear corrections (k_{h1})[22] for use in the GED refinements. (Methods used for each compound are described in the Supporting Information.)

Gas Electron Diffraction Measurements. Data were collected for **1–3** using the Edinburgh gas-phase electron diffraction apparatus.[23] An accelerating voltage of around 40 kV was used, representing an electron wavelength of approximately 6.0 pm. Scattering intensities were recorded on Kodak Electron Image films at nozzle-to-film distances and sample and nozzle temperatures given in Table S1. The weighting points for the off-diagonal weight matrices, correlation parameters, and scale factors for both camera distances for all compounds are given in Table S1. The electron wavelengths as determined from the scattering patterns for benzene, which were recorded immediately after the patterns for the sample compounds, are also included. The scattering intensities were measured using an Epson Expression 1680 Pro flatbed scanner and converted to mean optical densities as a function of the scattering variable, *s*, using an established program.[24] The data reduction and the least-squares refinement processes were carried out using the ed@ed program[25]> employing the scattering factors of Ross et al.[26]

Raman Spectroscopy. Raman spectra were recorded using a Jobin Yvon T64000 spectrometer equipped with a triple monochromator and a CCD camera. The samples were held in 1 mm glass capillary tubes and irradiated by 532 nm green light from a frequency-doubled Nd:YAG laser (DPSS model 532–20, 20 mW). Spectra were recorded in the solid state for **2**. Liquid spectra were recorded for pure samples of **1**, **2**, and **3** and solutions of **1** and **2**. A continuous-flow cryostat (Oxford Instruments OptistatCF using liquid nitrogen for cooling) was employed for the low-temperature measurements.

Results

Computational Methods. $Me_3GeGeMe_3$ (1). The PES of **1** was probed by scanning the torsional angle around the central Ge-Ge bond at the DFT/**A** and **A#**, DFT/**B**, MP2/**A**, and MP2/**B** levels of theory. A geometry optimization at the DFT/**C** level was also performed. In each case, a staggered structure was found to be the most favorable conformation

(18) *SAINTPLUS: Software Reference Manual*, version 6.45; Bruker-AXS: Madison, WI, 1997–2003.
(19) Blessing, R. H. *Acta Crystallogr. A* **1995**, *51*, 33–38; *SADABS*, version 2.1; Bruker AXS: Madison, WI, 1998.
(20) Sheldrick, G. M. *SHELX97, Programs for Crystal Structure Analysis*, release 97–2; Universität Göttingen: Göttingen, Germany, 1998.
(21) Frisch, M. J.; Trucks, G. W.; Schlegel, H. B.; Scuseria, G. E.; Robb, M. A.; Cheeseman, J. R.; Montgomery, J. A., Jr.; Vreven, T.; Kudin, K. N.; Burant, J. C.; Millam, J. M.; Iyengar, S. S.; Tomasi, J.; Barone, V.; Mennucci, B.; Cossi, M.; Scalmani, G.; Rega, N.; Petersson, G. A.; Nakatsuji, H.; Hada, M.; Ehara, M.; Toyota, K.; Fukuda, R.; Hasegawa, J.; Ishida, M.; Nakajima, T.; Honda, Y.; Kitao, O.; Nakai, H.; Klene, M.; Li, X.; Knox, J. E.; Hratchian, H. P.; Cross, J. B.; Bakken, V.; Adamo, C.; Jaramillo, J.; Gomperts, R.; Stratmann, R. E.; Yazyev, O.; Austin, A. J.; Cammi, R.; Pomelli, C.; Ochterski, J. W.; Ayala, P. Y.; Morokuma, K.; Voth, G. A.; Salvador, P.; Dannenberg, J. J.; Zakrzewski, V. G.; Dapprich, S.; Daniels, A. D.; Strain, M. C.; Farkas, O.; Malick, D. K.; Rabuck, A. D.; Raghavachari, K.; Foresman, J. B.; Ortiz, J. V.; Cui, Q.; Baboul, A. G.; Clifford, S.; Cioslowski, J.; Stefanov, B. B.; Liu, G.; Liashenko, A.; Piskorz, P.; Komaromi, I.; Martin, R. L.; Fox, D. J.; Keith, T.; Al-Laham, M. A.; Peng, C. Y.; Nanayakkara, A.; Challacombe, M.; Gill, P. M. W.; Johnson, B.; Chen, W.; Wong, M. W.; Gonzalez, C.; Pople, J. A. *Gaussian 03*, revision B.03; Gaussian, Inc.: Pittsburgh, PA, 2003.
(22) Sipachev, V. A. *J. Mol. Struct. (THEOCHEM)* **1985**, *22*, 143–151.
(23) Huntley, C. M.; Laurenson, G. S.; Rankin, D. W. H. *J. Chem. Soc., Dalton Trans.* **1980**, *6*, 954–957.
(24) Fleischer, H.; Wann, D. A.; Hinchley, S. L.; Borisenko, K. B.; Lewis, J. R.; Mawhorter, R. J.; Robertson, H. E.; Rankin, D. W. H. *Dalton Trans.* **2005**, *19*, 3221–3228.
(25) Hinchley, S. L.; Robertson, H. E.; Borisenko, K. B.; Turner, A. R.; Johnston, B. F.; Rankin, D. W. H.; Ahmadian, M.; Jones, J. N.; Cowley, A. H. *Dalton Trans.* **2004**, *16*, 2469–2476.
(26) Ross, A. W.; Fink, M.; Hilderbrandt, R. *International Tables for Crystallography*; Wilson, A. J. C., Ed.; Kluwer Academic Publishers: Dordrecht, The Netherlands, 1992; Vol. C, p 245.

Table 1. Calculated Geometric Parameters (Distances in pm, Angles in deg) of Ge_2Me_6 Obtained Employing Different Methods (See Theoretical Methods Above) and Refined Geometric Parameters for Ge_2Me_6 (Distances in pm, Angles in deg) from the SARACEN[27] GED study[a,b]

	method							
parameter	DFT/**A**[c]	DFT/**A#**[c]	DFT/**B**	MP2/**A**	MP2/**B**	MP2/**C**	GED (r_{h1})	GED restraint[d]
rGe−Ge	250.0	250.0	243.8	249.0	243.2	246.4	241.4(1)	
rGe−C	200.6	200.6	196.3	202.1	195.6	198.1	195.7(1)	
rC−H_{av}	109.7	109.5	109.5	110.6	109.5	109.0	110.4(3)	
∠Ge−Ge−C	110.9	110.4	110.6	110.8	110.1	110.8	110.3(1)	
∠Ge−C−H_{av}	110.4	110.3	110.6	110.5	110.6	110.5	112.4(4)	
φC(4)−Ge−Ge−C(19)	−51.1	−49.7	−58.4	−60.0	−60.0	−58.4	−59.3(14)	−59.2(15)
Me tilt							0.3(3)	0.3(3)

[a] Figures in parentheses are the estimated standard deviations of the last digits. [b] See text for parameter definitions. [c] The φC−Ge−Ge−C values are almost certainly artifacts of the computational method, with all other methods returning values of about −60°. [d] Obtained from the average torsion obtained by DFT/**B**, MP2/**A**, MP2/**B**, and MP2/**C**.

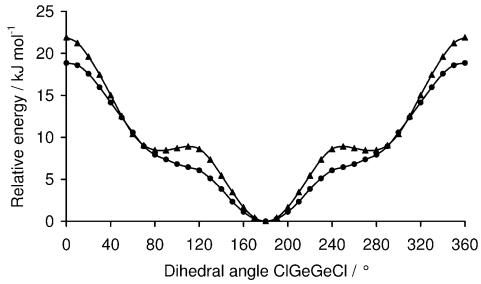

Figure 2. Torsion potential for $Me_2ClGeGeClMe_2$ (**2**) obtained employing DFT/**A#** (●) and MP2/**A#** (▲).

[see Figure S1 (Supporting Information Figure 1)]. The molecular structure of **1** with atom numbering is shown in Figure 1.

Generally, the calculated geometric parameters depend on the basis sets employed. Calculations at the DFT/**C** level gave a structure very similar to that obtained by DFT/**B**. Methods that include quasi-relativistic pseudopotentials for Ge (**A**, **A#**) tend to overestimate the GeGe bond length by about 8 pm compared to the gas-phase structure determined by GED. The GeC bond lengths are also calculated to be ∼5 pm longer. The use of relativistic triple-ζ basis sets (**C**) for Ge also tends to overestimate GeGe and GeC bonds by about 5 and 2 pm, respectively. The barrier to internal rotation was calculated employing DFT/**A** and MP2/**B**. For DFT/**A**, an eclipsed transition structure possessing D_{3h} symmetry was found, with a relative energy of 2.1 kJ mol^{-1}, representing the barrier to internal rotation. The barrier obtained with MP2/**B** is 5.8 kJ mol^{-1}, with the larger value resulting from the shorter computed GeGe bond. A summary of selected geometry parameters from different methods is given in Table 1.

$Me_2ClGeGeClMe_2$ (2). The PES for **2** was probed by rotating about the central Ge−Ge bond using mixed basis sets at the DFT/**A#** and MP2/**A#** levels. The antiperiplanar conformer was found to be the global minimum. However, a stable synclinal conformer was located, depending on the method employed. In Figure 2 the torsion potentials obtained with DFT/**A#** and MP2/**A#** are given. Although no synclinal minimum can be located with DFT/**A#**, the possible existence of a second stable conformer is indicated by a flat region in the potential curve. Employing MP2/**A#** led to the location of a second synclinal minimum.

Interestingly, employing all-electron or triple-ζ basis sets (**B**, **C**) also resulted in two minima being located on the PES of **2**. All calculated minima are summarized in Table 2. The stable antiperiplanar and synclinal conformers, located employing MP2/**B**, are shown in Figure 3.

As for **1**, the calculated geometric parameters depended on the method used. Selected parameters for **2** (antiperiplanar being referred to as conformer 1, synclinal as conformer 2) are given in Table 2. The SDD basis set overestimates the GeGe bond by 7 and 5 pm with B3LYP and MP2, respectively, compared to the experimental value of 243.7(5) pm. Employing basis sets **B** and **C** yields bond lengths in reasonable agreement with the experimental value.

The barrier for the synclinal to antiperiplanar transition is very small. The transition structure has a ClGeGeCl dihedral angle between 94 and 113°, depending on the method employed. Using MP2/**A#**, we calculated the barrier to be 0.5 kJ mol^{-1}, but with DFT/**B**, it is only 0.12 kJ mol^{-1}. The largest barrier is calculated with MP2/**B** as being 2.89 kJ mol^{-1}. This relatively large value results from the short GeGe bond length found with this method (see Table 2).

At about 20 kJ mol^{-1}, the barrier for the antiperiplanar to antiperiplanar transition is surprisingly large (see Figure 2), much larger than would be expected from the van der Waals radius of the chlorine atom, which is slightly smaller than for a methyl group (170–190 pm for Cl, 200 pm for Me). Therefore, the barrier height must be attributable to the small GeGeCl bond angle, which causes a large nonbonded Cl···Cl interaction in the transition state, characterized by φClGeGeCl = 0.0°. Depending on the method and basis set used, the nonbonded Cl···Cl distances are calculated to be between 377 and 400 pm, and GeGeCl angles widen to about 108°. The GeGe bond is somewhat lengthened in the transition state (246–252 pm), but this does not contribute much to the overall height of the energy barrier. The PES has been probed with respect to the GeGe bond length, with results shown in Figure 4. For both DFT/**A** and DFT/**B**, a distortion

(27) (a) Brain, P. T.; Morrison, C. A.; Parsons, S.; Rankin, D. W. H. *J. Chem. Soc., Dalton Trans.* **1996**, *24*, 4589–4596. (b) Blake, A. J.; Brain, P. T.; McNab, H.; Miller, J.; Morrison, C. A.; Parsons, S.; Rankin, D. W. H.; Robertson, H. E.; Smart, B. A. *J. Phys. Chem.* **1996**, *100*, 12280–12287. (c) Mitzel, N. W.; Rankin, D. W. H. *Dalton Trans* **1996**, *24*, 3650–3662.

(28) Draeger, M.; Ross, L. *Z. Anorg. Allg. Chem.* **1981**, *476*, 95–104.
(29) Draeger, M.; Ross, L. *Z. Anorg. Allg. Chem.* **1980**, *460*, 207–216.
(30) Parkanyi, L.; Kalman, A.; Sharma, S.; Nolen, D. M.; Pannell, K. H. *Inorg. Chem.* **1994**, *33*(1), 180–182.
(31) Weidenbruch, M.; Grimm, F.-T.; Herrndorf, M.; Schaefer, A.; Peters, K.; von Schnering, H. G. *J. Organomet. Chem.* **1988**, *341*, 335–343.
(32) Griffiths, J. E.; Walrafen, G. E. *J. Chem. Phys.* **1964**, *40*, 321–328.

Table 2. Geometric Parameters (Distances in pm, Angles in deg) and Relative Energies (kJ mol^{-1}) of $Me_2ClGeGeClMe_2$ (**2**) Obtained with Different Methods

	method						
parameter	DFT/**A**	DFT/**A#**	DFT/**B**	MP2/**A**	MP2/**A#**	MP2/**B**	DFT/**C**
conformer 1							
rGe−Ge	249.1	249.5	242.7	248.2	247.6	241.3	246.0
rGe−C_{av}	198.1	198.4	194.3	199.5	197.2	193.4	196.3
rGe−Cl	233.4	227.9	223.9	233.7	226.4	221.1	222.8
rC−H_{av}	109.6	109.4	109.4	110.4	109.4	109.4	108.9
∠Ge−Ge−C_{av}	114.8	114.3	113.6	114.5	114.1	113.1	114.2
∠Ge−Ge−Cl	102.1	103.1	102.9	102.6	102.5	102.4	103.5
∠Ge−C−H_{av}	109.8	109.8	110.0	109.9	110.2	110.0	109.8
φCl−Ge−Ge−Cl	180.0	180.0	180.0	180.0	180.0	180.0	180.0
E_{rel}/G_{rel}	0.0/0.0	0.0/0.0	0.0/0.0	0.0/0.0	0.0/0.0	0.0/0.0	0.0/0.0
conformer 2							
rGe−Ge			243.8		248.7	242.5	
rGe−C_{av}			194.6		197.5	193.7	
rGe−Cl			222.8		225.3	220.0	
rC−H_{av}			109.5		109.4	109.4	
∠Ge−Ge−C_{av}			113.6		114.0	113.9	
∠Ge−Ge−Cl			103.9		104.0	101.6	
∠Ge−C−H_{av}			110.0		110.1	110.0	
φCl−Ge−Ge−Cl			−78.0		−85.4	−69.4	
E_{rel}/G_{rel}			7.3/7.3		8.5/8.0	6.4/7.9	

Table 3. Experimental and Calculated Wavenumbers (cm^{-1}) of the Most Intense Lines in the Raman Spectrum of $Me_2ClGeGeClMe_2$ (**2**) in the Range of 200−650 cm^{-1}

		method					
		DFT/**B**		MP2/**A#**		MP2/**B**	
mode	experiment	antiperiplanar	synclinal	antiperiplanar	synclinal	antiperiplanar	synclinal
νGeGe	275	277	270	269	264	291	286
ν_sGeCl$_{i\text{-}ph}$	359	356	369	359	371	384	398
ν_sGeC$_2$	593	595	592	576	575	624	623

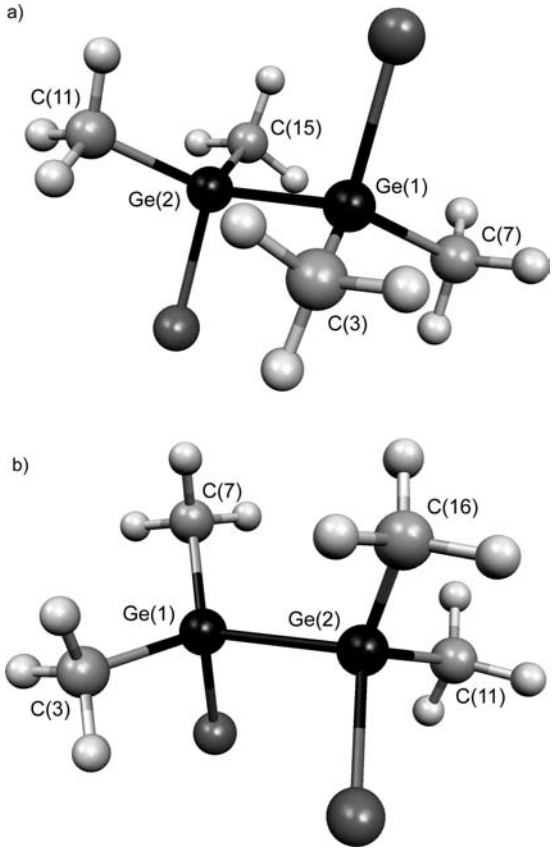

Figure 3. Molecular structures of the two observed conformers of $Me_2ClGeGeClMe_2$ (**2**) at the MP2/**B** level with atom numbering: (a) φCl−Ge−Ge−Cl = 180.0 ° and (b) φCl−Ge−Ge−Cl = −69.4°.

of the GeGe bond by 5 pm raises the energy by just 1 kJ mol^{-1}. An estimation of the potential energy with respect to the torsion around the GeGe bond can be derived from the geometry optimizations, where the variation of the ClGeGeCl dihedral angle of the synclinal conformer by 20° either side of the equilibrium position results in a maximum change of the relative energy of about 2 kJ mol^{-1}.

Calculation of vibrational frequencies was performed with DFT/**B**, MP2/**A#**, and MP2/**B**. Although the absolute wavenumbers vary with the different methods, the wavenumber differences between the two conformers for each vibration are almost identical (see Table 3). For νGeGe this difference was calculated to be 5−7 cm^{-1} between antiperiplanar and synclinal conformers. The difference in wavenumbers of the in-phase (i-ph) GeCl stretching mode, νGeCl$_{i\text{-}ph}$, is the largest

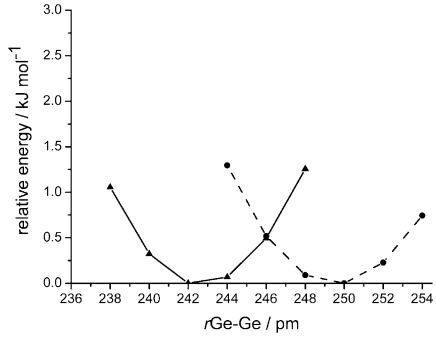

Figure 4. Dependence of the potential energy of $Me_2ClGeGeClMe_2$ (**2**) on the GeGe bond length obtained employing DFT/**A** (●) and MP2/**B** (▲). All other coordinates were allowed to optimize fully.

(12 to 14 cm^{-1}). Despite this large difference, no separate bands are expected in the Raman spectrum because of the small barrier between the conformers, which lies significantly below the Boltzmann energy at room temperature (2.4 kJ mol^{-1}). Therefore only an averaged spectrum is expected. The calculated wavenumber difference of the Raman-active symmetric GeC stretching mode, $\nu_s GeC_2$, is only 1−3 cm^{-1} between antiperiplanar and synclinal conformers.

$Me_2HGeGeHMe_2$ (3). The PES of **3** was probed with the DFT/**A**, DFT/**B**, MP2/**A**, and MP2/**B** methods. Calculations including the all-electron basis set **B** for Ge led to only one stable conformer, which has an almost eclipsed structure. It possesses C_2 symmetry with a HGeGeH dihedral angle of −110°. These results contradict the GED experiments, which clearly prove the existence of synclinal and antiperiplanar conformers in the gas phase.

The scans employing basis sets including relativistic effects for Ge (**A**, **A#**, and **C**) led to two minima, antiperiplanar and synclinal. With the DFT/**C** method, an antiperiplanar conformer was located as the global minimum on the PES; the synclinal conformer was found to be 2.3 kJ mol^{-1} higher in energy. These two minima, with atom numbering, are shown in Figure 5. Employing DFT with mixed basis sets, 6–31+G* for C and H and aug-cc-pVTZ-PP for Ge (in the following referred to as **C#**), gave very similar geometries and relative energies to those obtained with DFT/**C**. However, the computing time was considerably reduced. Therefore the frequency calculations to provide estimates of the amplitudes of vibration and curvilinear corrections for the GED refinement were performed using DFT/**C#**.

The barriers separating the minima are very small, as can be seen from Figure 6, which shows some torsion potentials. The barriers were calculated to be in the range from 0.6 (MP2/**A**) to 2.6 kJ mol^{-1} (DFT/**C#**). Again, these barriers are in the range of the Boltzmann energy at room temperature.

The predicted GeGe bond lengths depend heavily on the basis set employed. Using the all-electron basis set (**B**) gives GeGe bond lengths of about 244 pm for both DFT and MP2. Including quasi-relativistic effects and pseudopotentials with the SDD basis set gives longer bonds of about 249 pm (DFT/**A** and MP2/**A**). DFT/**C**, which includes relativistic triple-ζ basis sets, gives GeGe bond lengths of 245.1 pm for the antiperiplanar conformer and 245.3 pm for the synclinal conformer. The GeC bond lengths exhibit the same basis-set dependence as the GeGe bonds. Using SDD results in an overestimation of ∼4 pm, while the all-electron basis set predicts them to be a little shorter than determined in the gas phase by GED. The GeH bonds are overestimated slightly with all methods tested, except with basis set **C**, which gives a GeH bond length of about 155 pm. Some selected geometric parameters for the structures obtained with different methods are given in Table 4.

Frequencies were calculated employing DFT/**A**, MP2/**A**, and DFT/**C#** methods. The calculated wavenumbers of νGeGe, $\nu_s GeC_2$, and $\nu GeH_{i\text{-}ph}$ are given in Table 5. These three vibrations give the most intense lines in the Raman spectrum. From the small differences in calculated wavenumbers (∼3, 2, and 7 cm^{-1}, respectively), as well as the small barrier for conformer interconversion, no separated bands of the antiperiplanar and synclinal conformers are expected in the Raman spectrum.

GED Refinements. On the basis of the ab initio calculations described above, electron-diffraction refinements were carried out for **1–3**. A model with overall pseudo-C_2 symmetry to describe the gaseous structure of **1**, and models with two conformers, both of C_2 symmetry, were used to describe the gas-phase structures of **2** and **3**. See Supporting Information for a full description of the parameters.

The final refinements for **1–3** provided good fits to the data, with $R_G = 0.069$ ($R_D = 0.058$) for **1**, $R_G = 0.085$

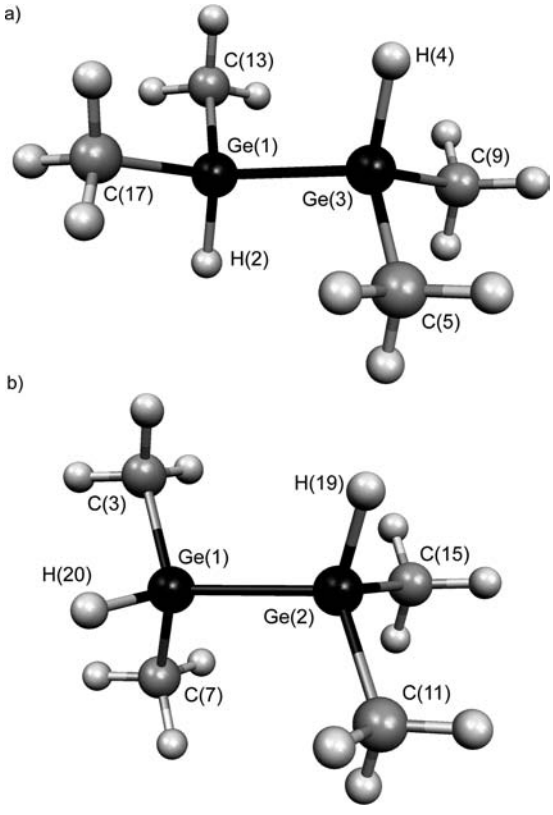

Figure 5. Molecular structures of the two conformers of $Me_2HGeGeHMe_2$ (**3**) at the DFT/**C#** level of theory with atom numbering: (a) φH−Ge−Ge−H = −179.9° and (b) φH−Ge−Ge−H = −67.3°.

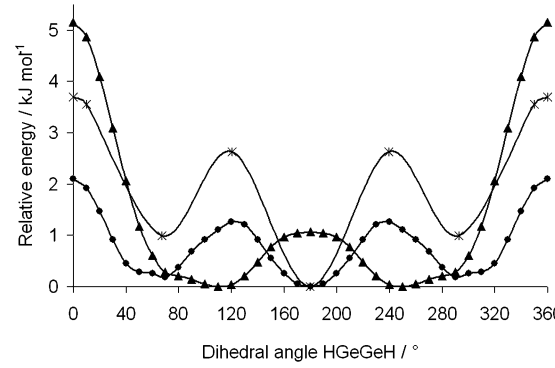

Figure 6. Torsion potential of $Me_2HGeGeHMe_2$ (**3**) obtained at the DFT/**A** (●), MP2/**B** (▲), and DFT/**C#** level of theory (×, only the relative energies of stationary points were calculated).

Table 4. Geometric Parameters (Distances in pm, Angles in deg) and Relative Energies (kJ mol^{-1}) of $Me_2HGeGeHMe_2$ (**3**) Obtained with Different Methods

	method					
parameter	DFT/**A**	DFT/**B**	MP2/**A**	MP2/**B**	DFT/**C**	DFT/**C#**
conformer 1						
rGe−Ge	249.2		248.7		245.3	245.1
rGe−C	200.2		201.9		197.8	197.8
rGe−H	156.8		157.3		154.3	155.1
rC−H_{av}	109.7		110.5		108.9	109.5
∠Ge−Ge−C	111.5		111.2		111.6	111.7
∠Ge−Ge−H	109.2		109.3		108.8	108.8
∠Ge−C−H_{av}	110.3		110.4		110.3	110.5
φH−Ge−Ge−H	−179.8		−179.8		−179.9	−179.9
E_{rel}/G_{rel}	0.0/0.0		0.2/0.0		0.0/0.0	0.0/0.0
conformer 2						
rGe−Ge	249.4	243.9	248.8	244.2	245.4	245.3
rGe−C	200.3	195.7	201.9	195.1	197.9	197.9
rGe−H	156.7	157.2	157.2	157.9	154.8	155.0
rC−H_{av}	109.7	109.6	110.5	109.5	108.9	109.5
∠Ge−Ge−C	111.7	110.6	111.0	111.1	111.8	111.8
∠Ge−Ge−H	108.8	108.3	109.8	108.6	108.6	108.6
∠Ge−C−H_{av}	110.3	110.7	110.4	110.6	110.3	110.5
φH−Ge−Ge−H	−68.3	−110.8	−73.5	−110.6	−67.3	−67.3
E_{rel}/G_{rel}	0.8/4.2	0.0/0.0	0.0/2.4	0.0/0.0	0.9/2.3	1.0/2.4

Table 5. Experimental and Calculated Wavenumbers (cm^{-1}) of the Most Intense Lines in the Raman Spectrum of $Me_2HGeGeHMe_2$ in the Range of 200−2100 cm^{-1}

		method					
		DFT/**A**		MP2/**A**		DFT/**C#**	
mode	experiment	antiperiplanar	synclinal	antiperiplanar	synclinal	antiperiplanar	synclinal
νGeGe	268	249	245	260	257	251	248
$\nu_s GeC_2$	584	556	558	558	560	563	565
$\nu GeH_{i\text{-}ph}$	2016	1980	1987	2011	2018	2054	2060

(R_D = 0.059) for **2**, and R_G = 0.091 (R_D = 0.058) for **3**. The radial-distribution curves for **1–3** are given in Figures 7−9 The molecular-scattering intensity curves are given in the Supporting Information (Figures S2−S4). Final refined parameters are listed in Tables 1, 6, and 7. The interatomic distances and corresponding rms amplitudes of vibration are given as supporting material in Tables S2−S4. The least-squares correlation matrices are given in Tables S5−S7, and the coordinates of the final refined structures from the GED investigation are given in Tables S8−S10.

Raman Spectroscopy. $Me_3GeGeMe_3$ (1). The vibrational frequencies and IR and Raman intensities were calculated at the DFT/**A#** and DFT/**B** levels, where the wavenumbers of the GeGe stretching mode, νGeGe, are calculated as 249/267 cm^{-1}, respectively. The Raman-active symmetric and asymmetric GeC stretching modes, $\nu_s GeC_3$ and $\nu_{as} GeC_3$, are 528/570 and 551/592 cm^{-1}, respectively. In the Raman spectrum, these bands are observed at 273, 573, and 588 cm^{-1}, in excellent agreement with the DFT/**B**

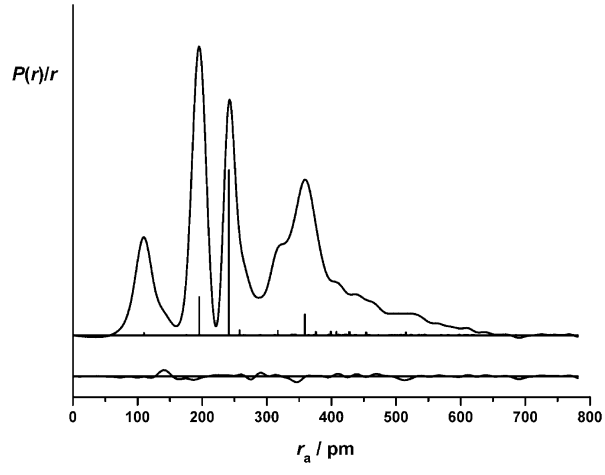

Figure 7. Experimental and difference (experimental − theoretical) radial-distribution curves, $P(r)/r$, for $Me_3GeGeMe_3$ (**1**). Before Fourier inversion the data were multiplied by $s\exp(-0.00002s^2)/(Z_{Ge} - f_{Ge})(Z_C - f_C)$.

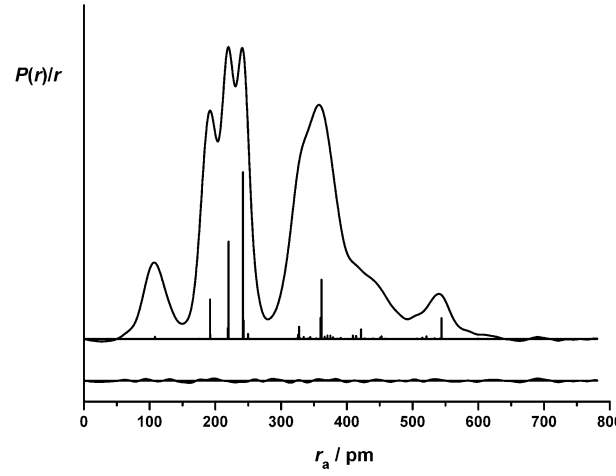

Figure 8. Experimental and difference (experimental − theoretical) radial-distribution curves, $P(r)/r$, for $Me_2ClGeGeClMe_2$ (**2**). Before Fourier inversion the data were multiplied by $s\exp(-0.00002s^2)/(Z_{Ge} - f_{Ge})(Z_{Cl} - f_{Cl})$.

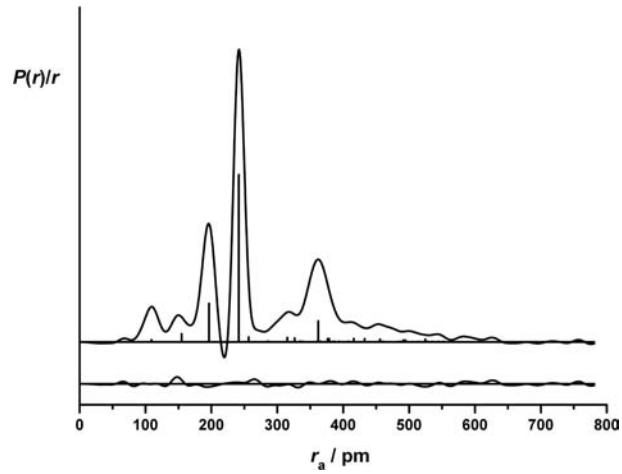

Figure 9. Experimental and difference (experimental − theoretical) radial-distribution curves, $P(r)/r$, for $Me_2HGeGeHMe_2$ (**3**). Before Fourier inversion the data were multiplied by $s \exp(-0.00002s^2)/(Z_{Ge} - f_{Ge})(Z_C - f_C)$.

results. Raman spectra of the pure liquid, as well as of solutions in THF and benzene, in the range of 200 –>700 cm^{-1} are shown in Figure 10. No differences between these spectra were observed.

$Me_2ClGeGeClMe_2$ (2). Raman spectra of the pure crystalline compound, as well as solutions in hexane and benzene, were recorded at different temperatures. The Raman spectrum of **2** in benzene solution is shown in Figure 11. The spectrum does not change at all within the temperature range of 265–293 K because of the small barriers separating the conformers.

An anticlinal conformation (also observed in the crystalline sample, see below) was observed by Raman spectroscopy. Four bands were observed in the range of GeC stretching vibrations from 560 to 640 cm^{-1} (see Figure 12), indicating the absence of an inversion center in the molecule. For the *eclipsed* structure (C_2, no inversion center), the selection rules predict four Raman-active bands in this region, while for the anti conformer (C_{2h}, including an inversion center), only two Raman-active bands are expected.

$Me_2HGeGeHMe_2$ (3). Raman spectra of pure liquid **3** were recorded at different temperatures, with the room temperature spectrum shown in Figure 13. The GeGe stretching mode, νGeGe, is observed at 268 cm^{-1} as a sharp line that shows no asymmetry, which would be expected if it consisted of two lines originating from antiperiplanar and synclinal conformers. Only an averaged spectrum, which does not change with temperature, is observed.

Crystal Structure Determination. $Me_2ClGeGeClMe_2$ (2). Two crystal structures of **2**, with $R = 0.028$ and 0.033, have been determined at temperatures of 100 and 223 K, respectively. Crystal data, structure refinement, and structural parameters are given in Table S11. An anticlinal structure was found at both temperatures, as shown in Figure 14. The central GeGe bond is found to be 242.1(1) pm long; the average GeCl bond length is 220.7(1) pm, and the average GeC bond length is 193.4(9) pm. In comparison, the GeGe bond length in Ge_6Ph_{12} has been determined to be 246.6 pm, and the dihedral angles are 49.2 and −48.9° [$R = 0.071$, room temperature (RT)].[28] In Ge_2Ph_6, the bond length is 243.7 pm ($R = 0.033$, RT).[29] A shorter GeGe bond of 241.9 pm was found in $Ph_3GeGeMe_3$ ($R = 0.036$, RT).[30] The longest GeGe bond has been detected in $Ge_2Bu^t_6$ (271.3 pm, $R = 0.028$, RT).[31]

For **2**, the GeGeCl angles are 104.8 and 105.8°, respectively. These small angles, which are also observed in the gas phase, may be explained by the tendency of germanium to become pentacoordinated, causing an attractive intramolecular interaction between a germanium atom and the vicinal chlorine atom. The CGeCl angles are also smaller than the tetrahedral angle (109.5°) with an average of 104.5°. Interestingly, the Cl(1)Ge(1)Ge(2)Cl(2) dihedral angle in the crystal is 124.4°, while the C(1)Ge(1)Ge(2)Cl(2) dihedral angle is only about 10°.

Discussion

Quantum chemical investigations of the conformational properties of methylated digermanes $Me_2XGeGeXMe_2$ (X = Me, Cl, or H) (**1**, **2**, and **3**) have been performed at different levels of theory. The potential-energy curves for internal rotation of all three compounds are characterized by shallow minima, which make accurate location and optimization difficult. However, sufficiently accurate results were obtained by probing the internal rotation with different methods and basis sets. Calculations employing basis sets that include quasi-relativistic or relativistic ECP's (basis sets **A**, **A#** and **C**, **C#**) generally give longer Ge−Ge, Ge−C, and Ge−Cl bond lengths than all-electron basis sets for the digermanes **1**–**3**. However, calculations employing triple-ζ basis sets (**C**, **C#**) give good agreement with experimentally determined values for these bond lengths. The calculated barriers for internal rotation of **1** and **3** are in the range of 2−5 kJ mol^{-1}. This is in reasonable agreement with the predictions for the barrier in digermane of about 6 kJ mol^{-1} estimated with vibrational spectroscopy.[32] For **2**, the antiperiplanar−synclinal barrier is in the same range. This is in direct contrast to the barrier for the antiperiplanar−antiperiplanar interconversion, via an eclipsed ClGeGeCl torsion, which is ∼20 kJ mol^{-1}. Despite the longer GeGe bond, the barrier is much larger than that reported for Si_2Cl_6, which is 4.2 kJ mol^{-1}.[33] The reason for this increased value is the tendency of fourth and higher row elements to become pentacoordinated in the presence of halogen atoms, in this case caused by an attractive intramolecular Ge···Cl interaction. It can be seen that, for these compounds, calculated structural parameters depend much more on the basis sets employed than is the case for the related C and Si systems, where no relativistic effects have to be considered.

The dependency of the results upon the basis set used is highlighted by the investigation of the potential-energy surface of **3**. Calculations with basis set **A** result in two minima, antiperiplanar and synclinal, in agreement with the GED experiment. The use of basis set **B** results in only one eclipsed conformer being observed, and the antiperiplanar conformer is predicted to be a maximum on the PES, albeit only ∼1 kJ mol^{-1}

(33) (a) Swick, D. A.; Karle, I. L. *J. Chem. Phys.* **1955**, *23*, 1499–1504. (b) Morino, Y.; Hirota, E. *J. Chem. Phys.* **1958**, *28*, 185–197.

Table 6. Refined and Calculated Geometric Parameters for $Me_2ClGeGeClMe_2$ (**2**) (Distances in pm, Angles in deg) from the SARACEN[27] GED Study[a,b]

number	parameter	MP2/**B** (r_e)	GED (r_{h1})	restraint
p_1	rC−H	109.4	108.7(3)	109.4(5)
p_2	rGe−C	193.4	192.0(2)	
p_3	rGe−Ge_{av}	241.9	242.7(2)	
p_4	rGe−Ge_{diff}	1.2	1.2(5)	1.2(5)
p_5	rGe−Cl_{av}	220.6	219.6(2)	220.6(10)
p_6	rGe−Cl_{diff}	1.1	0.9(5)	1.1(5)
p_7	∠Ge−C−H	109.9	109.8(4)	109.9(5)
p_8	∠Ge−Ge−C_{av}	113.6	112.7(6)	
p_9	∠Ge−Ge−C_{diff1}	2.2	2.2(5)	2.2(5)
p_{10}	∠Ge−Ge−C_{diff2}	2.8	2.8(5)	2.8(5)
p_{11}	∠Ge−Ge−Cl_{av}	102.0	103.1(3)	
p_{12}	∠Ge−Ge−Cl_{diff}	0.8	0.7(5)	0.8(5)
p_{13}	∠C−Ge−Cl (conformer 1)	106.6	105.4(7)	
p_{14}	∠C−Ge−Cl (conformer 2)	105.9	105.8(10)	105.9(10)
p_{15}	∠C−Ge−Cl (conformer 2)	106.3	106.2(10)	106.3(10)
p_{16}	φH(6)−C(3)−Ge(1)−Ge(2) (conformer 1)	62.8	62.7(24)	62.8(25)
p_{17}	φH(10)−C(7)−Ge(1)−Ge(2) (conformer 2)	−65.3	−65.3(25)	−65.3(25)
p_{18}	φH(6)−C(3)−Ge(1)−Ge(2) (conformer 2)	68.0	68.0(25)	68.0(25)
p_{19}	φCl(19)−Ge(1)−Ge(2)−Cl(20) (conformer 1)	180.0	179.9(20)	180.0(20)
p_{20}	φCl(15)−Ge(1)−Ge(2)−Cl(20) (conformer 2)	−69.4	−69.5(25)	−69.4(25)
p_{21}	fraction of conformer 1 in vapor [c]	0.95	0.90(fixed)	

[a] Figures in parentheses are the estimated standard deviations of the last digits. [b] See text for parameter definitions. [c] It was found that varying the torsion from −69.4° (MP2/**B**) to −85.4° (MP2/**A#**) made no difference to the goodness-of-fit factor; 0.90 was found to be the optimal amount of conformer 1 in the vapor. This was determined by a loop of the parameter value from 0.6 to 0.95 in steps of 0.05. This information, combined with the restraints needed to refine parameters relating to conformer 2, indicates that there is little information about conformer 2 contained within the data.

Table 7. Refined and Calculated Geometric Parameters for $Me_2HGeGeHMe_2$ (**3**) (Distances in pm, Angles in deg) from the SARACEN[27] GED Study[a,b]

number	parameter	DFT/**C#** (r_e)	GED (r_{h1})	restraint
p_1	rC−H	109.5	109.7(7)	
p_2	rGe−C	197.8	196.5(2)	
p_3	rGe−Ge	245.1	241.7(1)	
p_4	rGe−H	155.1	154.9(5)	155.1(5)
p_5	∠Ge−C−H	110.5	111.7(7)	110.5(10)
p_6	∠Ge−Ge−C	111.7	111.6(2)	
p_7	∠Ge−Ge−H	108.8	109.3(9)	108.8(10)
p_8	C−Ge−H	107.7	108.7(6)	107.7(10)
p_9	φH−C−Ge−Ge (conformer 1)	59.7	59.7(3)	
p_{10}	φH−Ge−Ge−H (conformer 1)	−179.9	−179.8(19)	−179.9(20)
p_{11}	φH−C−Ge−Ge (conformer 2)	58.5	58.5(19)	58.5(20)
p_{12}	φH−Ge−Ge−H (conformer 2)	−67.3	−67.3(19)	−67.3(20)
p_{13}	fraction of conformer 1 in the vapor	0.72	0.72(fixed)	

[a] Figures in parentheses are the estimated standard deviations of the last digits. [b] See Supporting Information for parameter definitions.

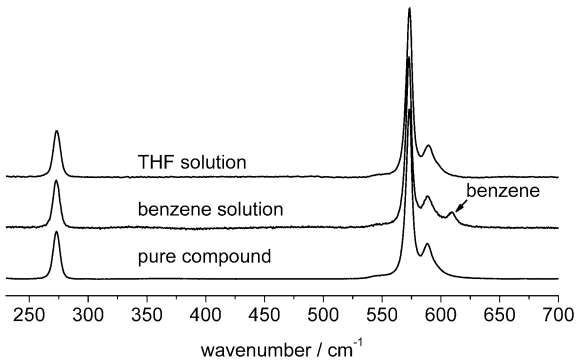

Figure 10. Raman spectra of $Me_3GeGeMe_3$ (**1**) at room temperature. The GeGe and GeC stretching vibrations between 200 and 700 cm^{-1} are shown.

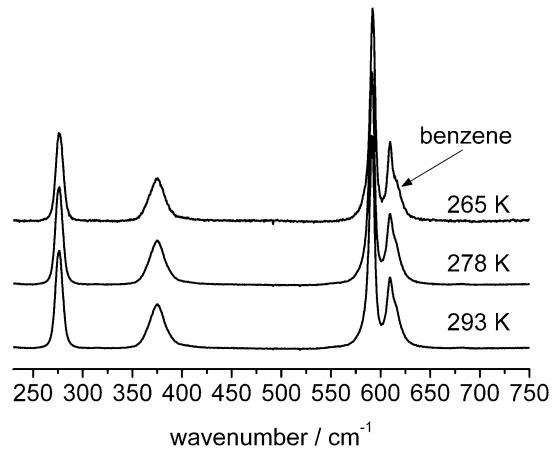

Figure 11. Raman spectra of $Me_2ClGeGeClMe_2$ (**2**) in benzene solution at different temperatures. The GeGe, GeCl, and GeC stretching vibrations between 250 and 750 cm^{-1} are shown.

higher in energy, which is well within the Boltzmann energy distribution at room temperature. Experimental structure data for compounds composed of fourth and higher row elements therefore are important for assessing the validity and quality of quantum chemical calculations.

Experimental investigations of **1**–**3** have been performed with Raman spectroscopy. As predicted by the calculations, the barriers for internal rotation are much smaller than those for their sila analogues. Contrary to the conformational analyses of SiC- and SiSi-containing systems, Raman spectroscopy is not able to resolve bands originating from different conformers

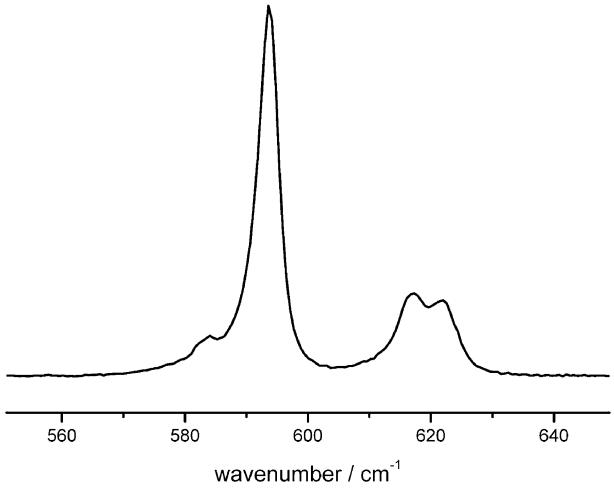

Figure 12. Raman spectrum of crystalline $Me_2ClGeGeClMe_2$ (**2**) at room temperature in the range of the GeC stretching vibrations (560−640 cm^{-1}).

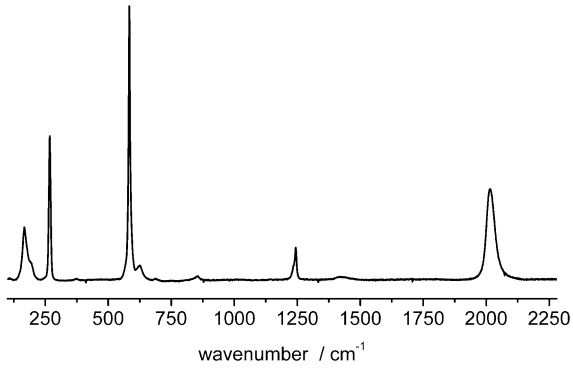

Figure 13. Raman spectrum of pure liquid $Me_2HGeGeHMe_2$ (**3**), recorded at room temperature. The region containing the GeGe, GeC, and GeH stretching vibrations (268/583/2015 cm^{-1}) is shown.

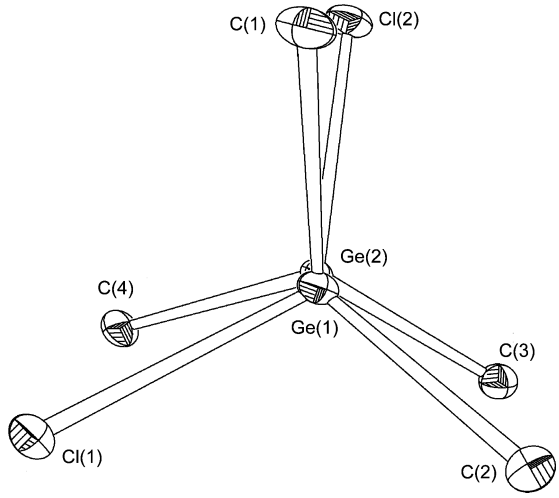

Figure 14. ORTEP plot (30% probability ellipsoids) of the molecular structure of $Me_2ClGeGeClMe_2$ (**2**), including atom numbering. Hydrogen atoms have been omitted for clarity.

of digermanes **1**–**3**. In these cases, the low barriers to rotation prevent the observation of separate conformers. However, the conformational equilibrium of permethylcyclohexagermane, where the barrier for the ring inversion is significantly larger because of concerted rotation about six Ge−Ge bonds, has been recently resolved with Raman spectroscopy.[15] Because the conformers could not be resolved by Raman spectroscopy, the conformational properties of **1**–**3** have also been probed by gas electron diffraction. Because GED has a time scale $\sim 10^7$ times faster than Raman spectroscopy, any additional conformers should be observable. One staggered structure is found in the gas phase for **1**. For **2**, two conformers were located by GED, antiperiplanar and synclinal, although the vapor consisted mainly of the antiperiplanar conformer (90%). For **3**, a mixture of synclinal and antiperiplanar conformers is also found in the gas phase, this time with 72% of the antiperiplanar conformer.

The high flexibility of these systems is underlined by the most interesting anticlinal solid-state molecular structure of **2**. In this structure, each chlorine ligand is eclipsed by a methyl group, a structure that was found to be a maximum on the potential-energy surface for the gaseous molecules. Therefore some strong intermolecular interactions must be present to outweigh the unfavorable atomic arrangement. Examination of the crystal structure indicates a widening of the angle between the methyl groups attached to germanium. This widening occurs at both ends of the molecule. The crystal packing indicates a reasonably close interaction between the chlorine and germanium atoms of adjacent molecules; the distance is 380 pm, compared to 375 pm for the sum of the van der Waals radii. There is also a strong intramolecular interaction between the chlorine and germanium atoms within the same molecule. The combined effect of these interactions may explain the eclipsed structure observed in the solid state.

A similar anticlinal molecular structure was found for solid $Me_2ClSnSnClMe_2$ (113 K, $R = 0.071$) with $\varphi ClSnSnCl = 128.0°$ The CSnSnCl dihedral angles are 21.5 and 122.1°, and at 99.4° and 102.3°, the ClSnSn angles are significantly smaller than tetrahedral.[34] Because of the intermolecular Sn···Cl interactions [324.0(3) and 329.2(3) pm], a double-chain structure with pentacoordinated Sn atoms is present in the crystal. However, no interactions stronger than van der Waals contacts were detected for **2**, and no crystal structure of the silicon analogue could be found in the literature but it may be presumed that no interactions stronger than van der Waals contacts would be observed for it either.

One may expect that this is purely caused by steric reasons, with the shorter Si−Si and Ge−Ge bonds preventing interaction between the chlorine of another molecule and the silicon or germanium. However, in the solid-state structures of far less crowded systems, such as Me_3SiCl, no interactions between Cl and Si are observed,[35] whereas the Sn analogue forms aggregates.[36] Hypercoordination around silicon and germanium is known, for example, H_3SiCl forms a Si···O interaction with dimethylether,[37] and Me_3GeCN forms infinite chains with Ge···N interactions.[38] Thus pentacoordination about silicon and germanium is clearly possible but

(34) Adams, S.; Draeger, M.; Mathiasch, B. *Z. Anorg. Allg. Chem.* **1986**, *532*, 81–89.
(35) Buschmann, J.; Lentz, D.; Luger, P.; Rottger, M. *Acta Crystallogr., Sect.C: Cryst.Struct. Commun.* **2000**, *56*, 121–122.
(36) Lefferts, J. L.; Molloy, K. C.; Hossain, M. B.; van der Helm, D.; Zuckerman, J. J. *J. Organomet. Chem.* **1982**, *240*(4), 349–361.
(37) Blake, A. J.; Cradock, S.; Ebsworth, E. A. V.; Franklin, K. C. *Angew. Chem.* **1990**, *102*(1), 87–89.
(38) Schlemper, E. O.; Britton, D. *Inorg. Chem.* **1966**, *5*, 511–514.

is not observed in the solid-state structure of **2**, with merely a close interaction between the germanium and silicon atoms of slightly more than the van der Waals radii.

One explanation for the minimal interactions in the solid-state structure of **2** (and the presumed lack of interaction in the silicon analogue) is the reduced atomic radii for silicon and germanium (~120 pm) in comparison with that of tin (~160 pm). The small atomic radii of silicon and germanium make them poorer acceptors than tin in general, and the acceptor properties are not enhanced by the presence of the electron-donating methyl groups. Another reason is that the donor to the coordination sphere is chlorine, which is not a good donor. Replacing chlorine with, for example, nitrogen or oxygen enhances the donor capabilities and leads to far stronger intermolecular interactions being observed.

Further work on the conformational properties of the related digermane $MeCl_2GeGeCl_2Me$ is currently being undertaken to observe the effect of replacing methyl groups with chlorine atoms.

Acknowledgment. M.H. and K.H. gratefully acknowledge the financial support by the "Fonds zur Förderung der wissenschaftlichen Forschung", Vienna (project P-17435). S.L.M. is grateful to the Royal Society of Edinburgh for a BP/RSE Research Fellowship and the EPSRC for funding for the electron diffraction (grant number EP/D057167). D.A.W. and H.E.R. thank the EPSRC for funding (EP/C513649).

Supporting Information Available: Tables listing the nozzle-to-plate distances, sample and nozzle temperatures (K), weighting functions (nm^{-1}), correlation parameters, scale factors, and electron wavelengths used in the gas electron diffraction, interatomic distances and amplitudes of vibration for the GED structures of **1**−**3**, least-squares correlation matrix for the GED refinement of **1**−**3**, experimental GED coordinates from the refinement of the pseudo-C_2 structure of **1**−**3**, and crystal data, structure refinement, and geometry parameters for **2** at 100 K and figures showing the torsional potential of **1**, experimental and final weighted difference molecular scattering intensities for **1**−**3**, and the GED parameter description for **1**−**3**. This material is available free of charge via the Internet at http://pubs.acs.org. Crystallographic data (excluding structure factors) for **2** have been deposited with the Cambridge Crystallographic Data Centre as supplementary publication no. CCDC 647136. Copies of the data can be obtained free of charge on application to The Director, CCDC, 12 Union Road, Cambridge, CB2 1EZ, U.K. [fax (internat.) +44 (0)1223 336033; e-mail deposit@ccdc.cam.ac.uk].

IC7018764